

---

# Interaction forces between oil–water particle interfaces— Non-DLVO forces

---

Raymond R. Dagastine,<sup>b</sup> Tam T. Chau,<sup>b</sup> D.Y.C. Chan,<sup>c</sup> Geoffrey W. Stevens<sup>b</sup> and Franz Grieser<sup>\*a</sup>

<sup>a</sup> School of Chemistry, Particulate Fluids Processing Center, University of Melbourne, Parkville, Victoria 3010 Australia. E-mail: franz@unimelb.edu.au; Fax: 61-3-93475180; Tel: 61-3-83446476

<sup>b</sup> Department of Chemical Engineering and Biomolecular Engineering, Particulate Fluids Processing Center, University of Melbourne, Parkville Victoria 3010 Australia

<sup>c</sup> Department of Mathematics and Statistics, Particulate Fluids Processing Center, University of Melbourne, Parkville, Victoria 3010 Australia

Received 20th April 2004, Accepted 28th May 2004

First published as an Advance Article on the web 5th October 2004

The interaction force between a rigid silica sphere and a butyl or octyl acetate droplet was measured in an aqueous environment using atomic force microscopy (AFM). The force measurements were performed without added stabilizers and the observed force behavior was found to be dependent on the type of inorganic electrolyte present, where the interfacial tension was constant over the electrolyte concentration range used. Force measurements in the presence of sodium nitrate showed repulsion at all concentrations. Force measurements in the presence of calcium nitrate or sodium perchlorate exhibited an initial repulsion followed by an attraction resulting in a mechanical instability in the AFM cantilever, termed jump-in. The force behavior observed was independent of the water solubility of the organic liquid, in that the same force–distance characteristics were obtained for slightly water soluble butyl acetate and the water sparingly soluble octyl acetate droplets. Modeling of the drop profile during particle–droplet interactions for this type of AFM measurement showed that the force–distance data for the sodium nitrate system obeys typical DLVO interactions. The disagreement between the DLVO predictions for the sodium perchlorate and calcium nitrate systems is attributed to a specific ion effect at the liquid–liquid interface, which gives rise to an attraction force that is greater than the electrostatic double layer repulsion over the length scale of 5 to 10 nm.

---

## Introduction

The study of the interaction forces between liquid–liquid or liquid–vapor interfaces has been of interest for quite some time. Experimental approaches have employed a variety of methods. They have ranged from the classical measurements of Derjaguin *et al.*<sup>1</sup> to study the disjoining pressure of thin films, to more recent methods developed for studying rigid systems, and now extended to deformable systems. These later techniques include total internal reflection microscopy, a modified

surface forces apparatus,<sup>2,3</sup> alignment of droplets in magnetic fields<sup>4,5</sup> and atomic force microscopy (AFM).<sup>6–20</sup> All of these measurements are motivated by the study of how the structure of the molecules at liquid interfaces mediates the interaction forces between liquid–liquid or liquid–vapor interfaces. Understanding the interaction forces between liquid interfaces leads to insight into the properties of complex fluids commonly encountered in industrial applications. They include formulation, stability, and rheological properties of emulsions in areas such as food processing or the control of drop coalescence times in solvent extraction processes for applications as diverse as hydrometallurgy and pharmaceutical processing.

The present work uses AFM to study the interaction forces between silica spheres and the liquid–liquid interface of polar organic liquids in aqueous solution (see Fig. 1). This study is motivated by an earlier drop coalescence study between organic liquid drops in water. The previous work of Stevens *et al.*<sup>21</sup> investigated the effect of inorganic electrolytes on the coalescence times of organic liquid drops in water; the coalescence times were shown to increase for polar liquids, such as butyl acetate, whereas the coalescence times were independent of electrolyte concentration for non-polar liquids. The rate-limiting step in drop coalescence is commonly the film drainage between the interfaces where viscosity and surface tension have been shown to be crucial parameters for flow and interfacial deformation, respectively, as revealed by both theoretical and experimental studies (to name a few<sup>22–25</sup>). Interaction forces are significant to the thinned-film stability prior to rupture. Stevens *et al.*<sup>21</sup> concluded that a repulsive force helped to stabilize the polar organic liquids during coalescence. Furthermore, whereas electrophoresis measurements showed the droplets were charged, the origin of the force was not expected to be from an electrostatic double layer (EDL). An EDL force would be screened by the addition of electrolytes. This effect would result in a decrease in coalescence times, yet increases in the coalescence times were observed. Stevens *et al.*<sup>21</sup> suggested possible origins of the repulsive force as being due to increases in interfacial viscosity or an effect due to solvent structure or ordering at the liquid–liquid interface due to the polar nature of the organic liquids.

The extension of colloidal probe AFM (first developed by Ducker *et al.*<sup>26</sup> and Butt *et al.*<sup>27</sup> for rigid surfaces) to deformable interfaces has an added difficulty in the force analysis, due to interface deformation at close approach of the surfaces. The data analysis methods for rigid systems are not applicable to deformable surfaces.<sup>10,11,14</sup> In the analysis for rigid systems, measurement of force *versus* motion of the piezo distance actuator is converted to force *versus* intersurface separation. For this to be accomplished in deformable systems, one must separate the effects of interface deformation from changes in the interaction forces. A number of theoretical studies have examined this type of measurement and proposed several methods to analyze this type of data.<sup>10–12,14,16,19,20,28</sup> All the approaches involve modeling the deformation of the interface *via* the Young–Laplace equation where the drop shape is perturbed by the presence of the rigid probe. The drop size employed in the AFM experiments is typically below the capillary length of the system, thus surface tension and surface forces govern the interface shape where the effects of gravity are

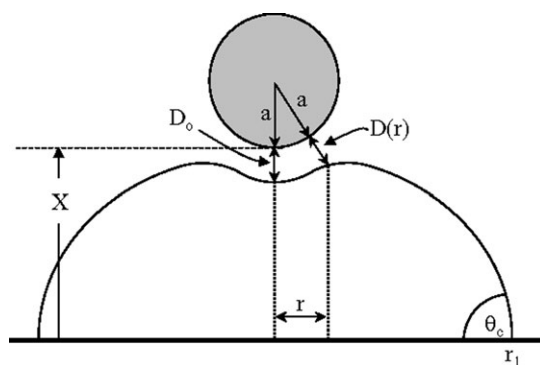


**Fig. 1** A schematic (not to scale) of the AFM experiment between a rigid silica sphere and an oil droplet immobilized on a surface. Note: the deformation is exaggerated and only on the order of 100 nm to 200 nm.

negligible. The capillary length,  $\lambda$ , is defined as

$$\lambda = \left( \frac{\gamma}{\Delta\rho g} \right)^{1/2} \quad (1)$$

where  $g$  is gravity,  $\gamma$  is interfacial tension of the fluid interface and  $\Delta\rho$  is the difference in density between the fluid phases.<sup>10</sup>

Previous work has measured the forces between silica probes and non-polar liquids (such as decane<sup>8,18</sup> and hexadecane<sup>11</sup>) in the presence of aqueous inorganic electrolyte solutions. The force behavior showed an EDL repulsion followed by a short range van der Waals attraction leading to either engulfment or formation of a three phase contact line with the silica bead and droplet. Both the silica surface and the oil drop were charged and the overall force behavior could be explained using DLVO theory,<sup>29,30</sup> where the total potential energy is defined as the sum of the repulsive and attractive components from EDL and van der Waals forces. In the present study colloidal probe AFM is used to directly probe the interaction between a rigid silica sphere and a droplet (a spherical cap of oil in water immobilized on a surface, see Fig. 1) of a polar organic liquid immersed in aqueous salt solutions. The polar liquids, butyl and octyl acetate, have been examined in a series of inorganic electrolytes. The observed interaction forces follow the expected DLVO type force model for sodium nitrate, but a non-DLVO attraction is observed for sodium perchlorate and calcium nitrate regardless of the polar organic liquid used.

## Methods

A Digital Instruments Multimode AFM and Nanoscope IIIa AFM controller were used for all experiments. Silica particles with a diameter of 5  $\mu\text{m}$  were attached to Thermomicroscopes Microlevers (Digital Instruments) AFM cantilevers.<sup>26</sup> Cantilever spring constants were measured according to the method of Hutter and Bechhoefer<sup>31</sup> and ranged between 0.025 to 0.081  $\text{N m}^{-1}$ . The inorganic salts used in these experiments were sodium nitrate (BDH), calcium nitrate (Ajax Chemicals), and sodium perchlorate (Ajax Chemicals). All glassware was bathed in surfactant cleaning solution for 1 h followed by 1 h in 10% nitric acid. Butyl acetate (Aldrich Chem. Co.) and octyl acetate (Aldrich Chem. Co.) were used as the oil droplet immobilized on a Melinex polymer film (semicrystalline PET film with no additives) according to the procedure outlined in Dagastine *et al.*<sup>12</sup> All measurements were performed with either butyl or octyl acetate saturated aqueous solutions. The colloidal probe was centered above the oil droplet (spherical caps with radii of the order of 100  $\mu\text{m}$  to 300  $\mu\text{m}$ ) *via* transitional stages and then positioned above the droplet, first using the course stepping motor, and then using the piezo tube for fine control. Force curves (an approach and retract force–distance cycle) were taken at a series of approach speeds (100  $\text{nm s}^{-1}$  to 2  $\mu\text{m s}^{-1}$ ), but no dependence of the force curve on the speed was observed. At the end of the experiments, the cantilever was pressed onto the underlying substrate to determine the detector sensitivity of the AFM photodiode. The radius of the spherical cap,  $r_1$ , was measured from above with a CCD camera to an accuracy of 5  $\mu\text{m}$ . The undistorted radius of the drop,  $R_0$ , was calculated according to  $\sin \theta_c = r_1/R_0$ , where the contact angle,  $\theta_c$ , and  $r_1$  are defined in Fig. 1.

The AFM photodiode voltage was converted to cantilever deflection,  $\Delta d$ , using the detector sensitivity determined at the end of the experiment and then converted to force *via*  $F = k_c \Delta d$ , where  $k_c$  is the spring constant of the cantilever. A simple distance balance of the AFM measurement shows that the piezo motion,  $\Delta l$ , is equal to the changes in deflection,  $\Delta d$ , separation,  $\Delta D$ , and deformation,  $\Delta z$ , of the system.<sup>10,11,14</sup> Using this distance balance, the deflection was subtracted from the piezo motion leading to

$$\Delta X = \Delta l - \Delta d \quad (2)$$

where  $\Delta X$  is the change in separation distance and deformation. Defined in Fig. 1,  $X$  is the distance from the bottom of the sphere to the top of the substrate. The definition of  $X$  is somewhat arbitrary because only changes in  $\Delta X$  are measured and an absolute measure of the distance  $X$  is not known. It is standard practice to set an origin for  $X$  and display  $F(\Delta X)$  relative to this origin.<sup>10,14</sup> In this respect, the curves have been shifted for convenience to clearly show specific features.

Interfacial tension was measured using the pendant drop method with a DataPhysics OCA 20 Tensiometer and axisymmetric drop shape analysis software. Sessile drop contact angle

measurements were made using the same system. Solubility measurements of butyl acetate in different electrolyte solutions were measured using a Varian UV-Spectrophotometer. The measured molar absorptivity of butyl acetate was  $53.4 \text{ M}^{-1} \text{ cm}^{-1}$  at a wavelength of 202 nm.

## Results

Independent physico-chemical characterization of the drop properties is required for the quantitative analysis of the force curves. The interfacial tension for butyl acetate and octyl acetate were determined as  $13.5 \text{ mN m}^{-1}$  and  $19.6 \text{ mN m}^{-1} \pm 0.5 \text{ mN m}^{-1}$ , respectively, and were found to be independent of both the type of inorganic electrolyte and the electrolyte concentration over the range used in this study. The droplet contact angle on Melinex film was measured independently to be  $140^\circ \pm 2^\circ$  using the sessile drop method. Butyl acetate is slightly soluble in water (measured to be 58.5 mM in MilliQ water at saturation), while octyl acetate is sparingly soluble. The solubility of butyl acetate decreases as expected to 7.18, 4.7 and 0.58 mM at 1 mM sodium nitrate, calcium nitrate, and sodium perchlorate, respectively.

The interaction between a silica sphere and a butyl acetate droplet in the presence of sodium nitrate solutions is shown in Fig. 2. The same cantilever and probe were used for each curve, but three different drops of similar radii ( $\sim 300 \mu\text{m}$ ) were employed. Butyl acetate is slightly soluble in water and whereas all experiments were done in saturated solutions, the solubility of a curved droplet is enhanced by the increased Laplace pressure. This results in droplets that are stable over the course of 30 to 60 min, but not stable over long enough times to perform measurements for a range of electrolyte concentrations. As discussed above,  $\Delta X$  is not the intersurface separation distance, thus the relative curve positions are not informative and have been spaced to show changes in force structure.

The range of the repulsion at low forces decreases with increasing ionic strength, as expected for an EDL force. EDL repulsive forces follow an approximate exponential form where the characteristic decay length, the Debye length,  $\kappa^{-1}$ , can be calculated based on solution ionic strength or regressed from a plot of the natural logarithm *versus* surface separation.<sup>32</sup> The natural logarithm for the force *versus*  $\Delta X$  is displayed in the inset; where the limiting slope was compared to the expected

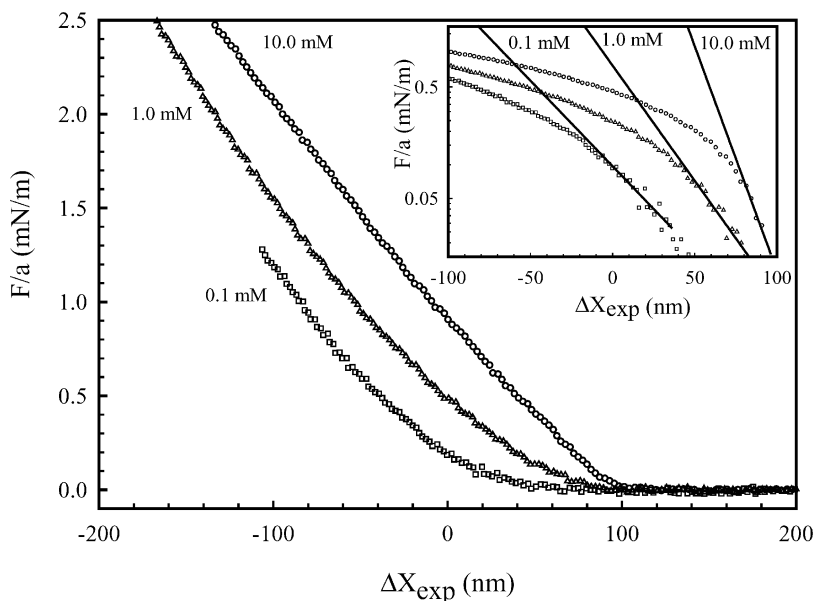


**Fig. 2** The measured interaction force,  $F$ , *versus* relative piezo motion,  $\Delta X_{\text{exp}}$ , between a silica sphere (with radius,  $a = 2.5 \mu\text{m}$ ) and an immobilized butyl acetate droplet on a surface in the presence of sodium nitrate ( $\text{NaNO}_3$ ) measured using AFM. The inset shows the logarithm of the force curves where the limiting slopes, marked by the solid line, are given in Table 1.

**Table 1** The regressed slopes from the insets of Figs. 2–4 compared to the expected Debye length,  $\kappa^{-1}$ , based on solution ionic strength

Concentration/ mM	$\kappa^{-1}/\text{nm}$ (NaNO <sub>3</sub> )	$\kappa^{-1}/\text{nm}$ (NaClO <sub>4</sub> )	$\kappa^{-1}/\text{nm}$ (Theory, 1 : 1)	$\kappa^{-1}/\text{nm}$ (Ca(NO <sub>3</sub> ) <sub>2</sub> )	$\kappa^{-1}/\text{nm}$ (Theory, 2 : 1)
0.1	26.8	26.7	30.4	15.5	17.6
1.0	17.0	15.4	9.6	16.4	5.6
10.0	9.6	7.7	3.04	—	—

ionic strengths given in Table 1. The large disagreement in the regressed  $\kappa^{-1}$  values is due to interfacial deformation because the distance  $\Delta X$  is a nonlinear function of intersurface separation.<sup>10,12</sup> Only repulsion was observed in the force measurements in sodium nitrate solution over a large range of the piezo drive distance. This behavior was *only* observed for sodium nitrate solutions.

The interaction force between butyl acetate droplets in the presence of sodium perchlorate and calcium nitrate are shown in Figs. 3 and 4, respectively. The range of the repulsion follows the same behavior as above for the decay lengths of force *versus*  $\Delta X$ . The notable difference from the sodium nitrate case is the presence of an attractive force resulting in the termination of the force curve denoted with arrows in Figs. 3 and 4. The termination of the force curve is a consequence of a process referred to as “jump-in”. Here, the gradient of the force curve exceeds the spring constant of the cantilever causing a mechanical instability, where the dynamics of the jump-in process are faster than the sampling rate of the AFM. Therefore, this point is the termination of the measurement. Attraction was observed intermittently for the sodium perchlorate results in Fig. 3 for the lowest concentration of 0.1 mM. This is consistent with previous results on non-polar liquids where jump-in is not always observed at low ionic strengths.<sup>8,18</sup> At all higher concentrations of sodium perchlorate and all cases for calcium nitrate the force curves all terminate in jump-in.

The results for octyl acetate for the same three inorganic electrolytes (sodium nitrate, sodium perchlorate and calcium nitrate) are given in Figs. 5–7. While octyl acetate is still polar it is sparingly

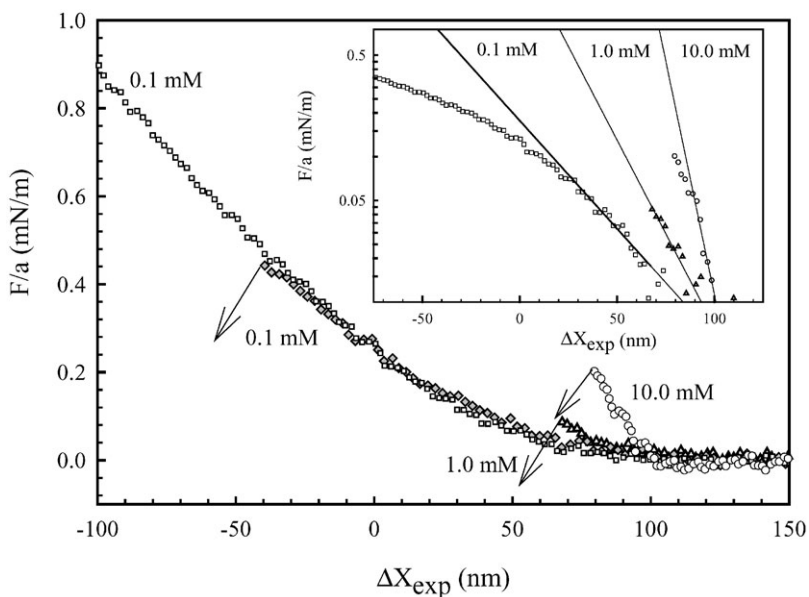


**Fig. 3** The measured interaction force,  $F$ , versus relative piezo motion,  $\Delta X_{\text{exp}}$ , between a silica sphere (with radius,  $a = 2.5 \mu\text{m}$ ) and an immobilized butyl acetate droplet on a surface in the presence of sodium perchlorate (NaClO<sub>4</sub>) measured using AFM. The inset shows the logarithm of the force curves where the limiting slopes, marked by the solid line, are given in Table 1.

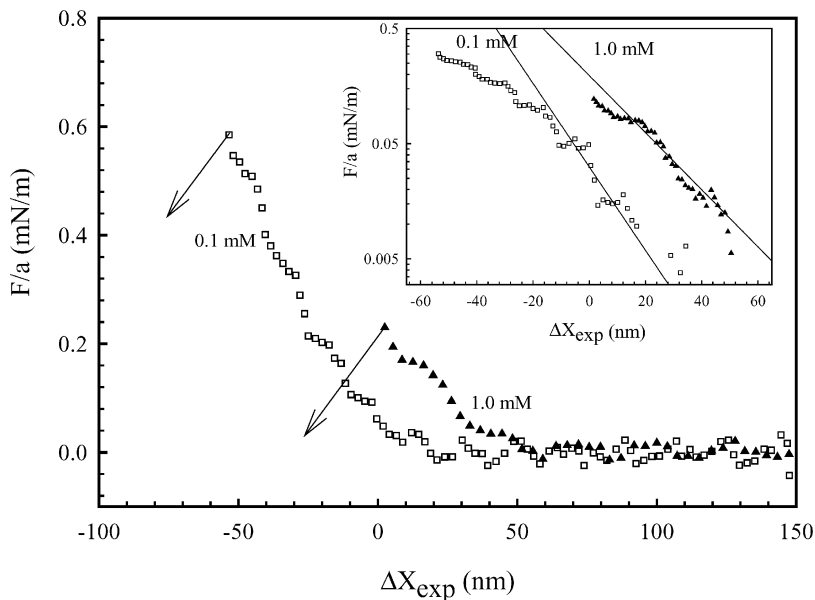


**Fig. 4** The measured interaction force,  $F$ , versus relative piezo motion,  $\Delta X_{\text{exp}}$ , between a silica sphere (with radius,  $a = 2.5 \mu\text{m}$ ) and an immobilized butyl acetate droplet on a surface in the presence of calcium nitrate ( $\text{Ca}(\text{NO}_3)_2$ ) measured using AFM. The inset shows the logarithm of the force curves where the limiting slopes, marked by the solid line, are given in Table 1.

soluble in water, thus the immobilized drops are stable over the course of hours and all the data for each electrolyte was taken on the same drop with sizes of  $200 \mu\text{m}$  to  $300 \mu\text{m}$ . Only a repulsive

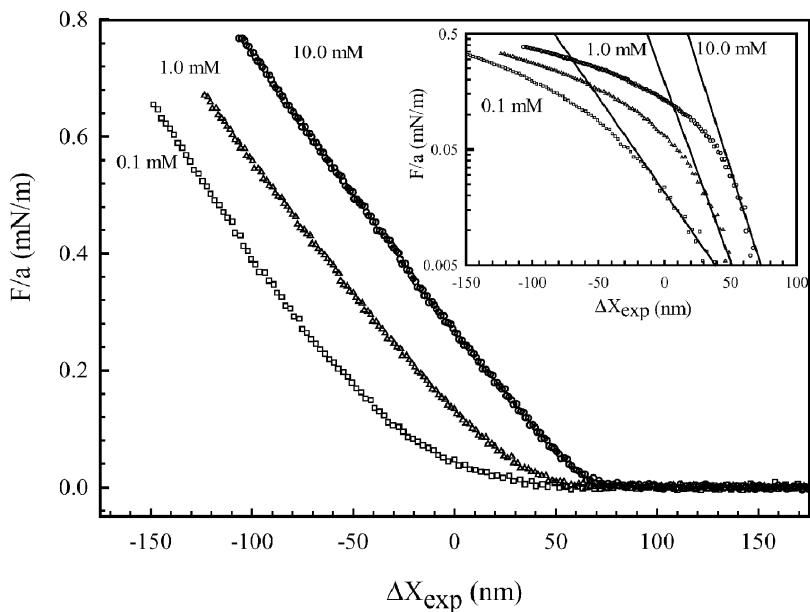


**Fig. 5** The measured interaction force,  $F$ , versus relative piezo motion,  $\Delta X_{\text{exp}}$ , between a silica sphere (with radius,  $a = 2.5 \mu\text{m}$ ) and an immobilized octyl acetate droplet on a surface in the presence of sodium nitrate ( $\text{NaNO}_3$ ) measured using AFM. The inset shows the logarithm of the force curves where the limiting slopes, marked by the solid line, are given in Table 2.

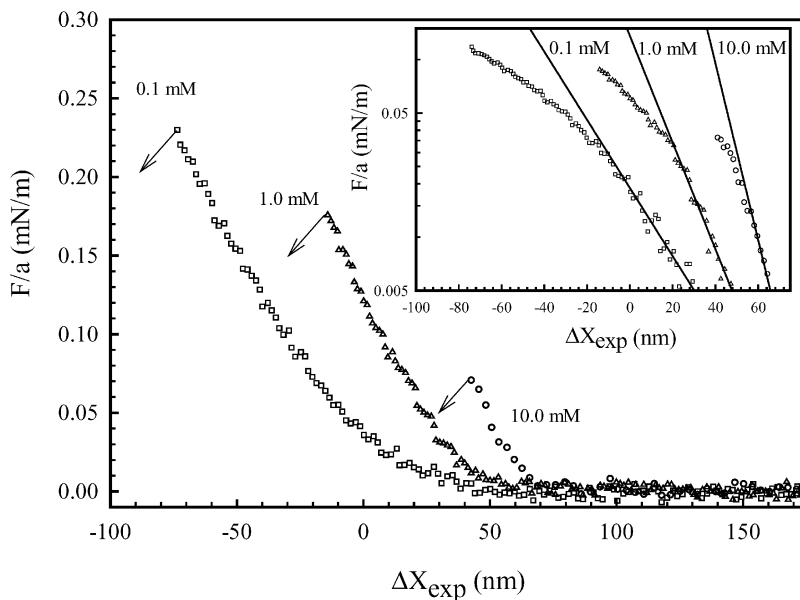


**Fig. 6** The measured interaction force,  $F$ , versus relative piezo motion,  $\Delta X_{\text{exp}}$ , between a silica sphere (with radius,  $a = 2.5 \mu\text{m}$ ) and an immobilized octyl acetate droplet on a surface in the presence of sodium perchlorate ( $\text{NaClO}_4$ ) measured using AFM. The inset shows the logarithm of the force curves where the limiting slopes, marked by the solid line, are given in Table 2.

interaction was observed in the presence of sodium nitrate shown in Fig. 5 and the range of the repulsion at low forces again scales with ionic strength. Initial repulsion followed by jump-in was observed for all concentrations with the remaining two electrolytes in Figs. 6 and 7. Again, the range

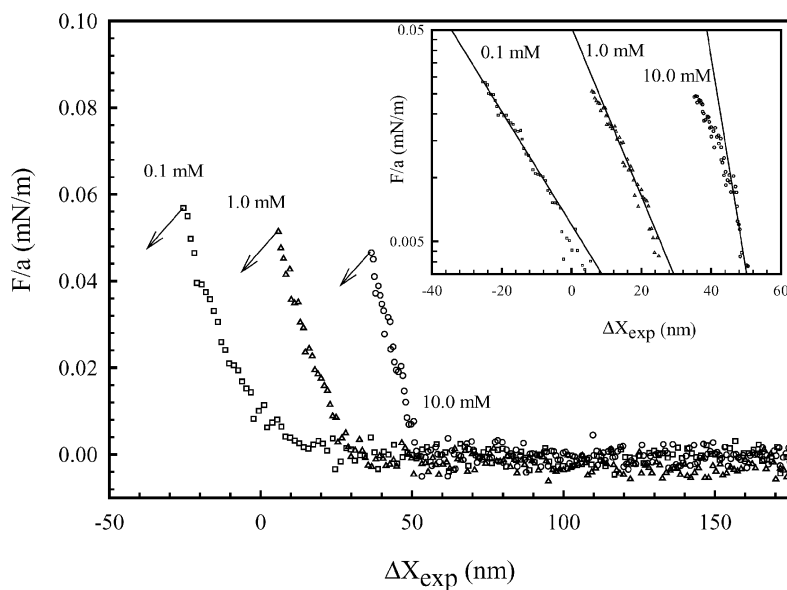


**Fig. 7** The measured interaction force,  $F$ , versus relative piezo motion,  $\Delta X_{\text{exp}}$ , between a silica sphere (with radius,  $a = 2.5 \mu\text{m}$ ) and an immobilized octyl acetate droplet on a surface in the presence of calcium nitrate ( $\text{Ca}(\text{NO}_3)_2$ ) measured using AFM. The inset shows the logarithm of the force curves where the limiting slopes, marked by the solid line, are given in Table 2.

**Table 2** The regressed slopes from the insets of Figs. 5–7 compared to the expected Debye length,  $\kappa^{-1}$ , based on solution ionic strength

Concentration/ mM	$\kappa^{-1}/\text{nm}$ (NaNO <sub>3</sub> )	$\kappa^{-1}/\text{nm}$ (NaClO <sub>4</sub> )	$\kappa^{-1}/\text{nm}$ (Theory, 1 : 1)	$\kappa^{-1}/\text{nm}$ (Ca(NO <sub>3</sub> ) <sub>2</sub> )	$\kappa^{-1}/\text{nm}$ (Theory, 2 : 1)
0.1	23.4	21.5	30.4	15.5	17.6
1.0	11.7	14.6	9.6	11.0	5.6
10.0	11.0	7.7	8.0	4.1	1.8

of the repulsion at low forces scaled with ionic strength and the regressed limiting slopes of the logarithm of the force *versus*  $\Delta X$ , do not correlate with the expected Debye length as shown in Table 2.

## Discussion

The above force data show a clear dependence on the type of electrolyte present in solution where all other variables appear to be constant. The interfacial tension and contact angle are independent of the type and concentration of the electrolyte. The undistorted drop radii are similar and theoretical analysis has shown that the force is not very sensitive to the variation of the drop radii used in these experiments.<sup>12</sup> The oil solubility does not appear to result in any difference in the force behavior.

The only variable unaccounted for is the surface force between the interfaces, which appears to be electrolyte dependent. To propose that one of the above force–separation behaviors (attraction or continued repulsion) is due to a non-DLVO force requires a convincing description of what is the expected DLVO behavior. In order to address this issue a semi-analytical model developed for analysis of this type of AFM measurement is used to predict the force curve, *i.e.*  $F(\Delta X)$ , where *a priori* knowledge of the disjoining pressure is required for this calculation.<sup>10,17,19</sup> This is a semi-quantitative approach to demonstrate the expected DLVO force behavior for the system in question. This treatment is separated into three parts. First a description of the physical situation required for either jump-in or repulsion only are explained in terms of the drop deformation and DLVO interaction forces. Second, using literature estimates for the surface potential for the silica and butyl acetate surfaces the force curves in this study are predicted based on a DLVO force model. Finally, the model results are compared to the experimental measurements to determine whether or not the force behavior follows a DLVO force model.

### Jump-in or wrapping

An in-depth theoretical analysis of the occurrence of jump-in or alternatively, “wrapping” can be found in Dagastine and White,<sup>19</sup> only the relevant points for discussion are summarized here. As mentioned above, jump-in occurs from an attractive force, which leads to a mechanical instability in the cantilever. If jump-in does not occur irrespective of the amount of deformation in the droplet, a different physical situation occurs referred to as wrapping. When wrapping occurs, a film of effectively constant thickness, is maintained between the two interacting interfaces. This can be shown analytically by describing the gap between the interfaces, where the disjoining pressure is significant, according to:<sup>10</sup>

$$\left. \begin{aligned} D'' + \frac{1}{t}D' - \left(2\left(1 + \frac{a}{R_0}\right) - \frac{a\Pi(D)}{\gamma}\right)D_0 &= 0 \\ D(0) = D_0 \quad D'(0) &= 0 \end{aligned} \right\} \quad (3)$$

where  $a$  is the particle radius,  $\Pi(D)$  is the disjoining pressure, and  $D(t)$  is intersurface separation, and  $t$  is the radial distance in dimensionless form ( $t = r/(aD_0)^{1/2}$ ). When predicting the force curve, the above equation is solved numerically, but it reduces to a constant ( $D(t) = D_w$ ) if the disjoining pressure satisfies the condition

$$\Pi(D_w) = 2\gamma\left(\frac{1}{a} + \frac{1}{R_0}\right) \quad (4)$$

This condition is easily satisfied if the disjoining pressure has a large short-range force and the interface is sufficiently pliable. If this is true, instead of the two interfaces becoming closer, the observed increase in force is primarily from the deformation of the drop, and an increase in the interaction area.

The next step is to understand how changing parameters in a disjoining pressure using a DLVO force model results in wrapping or jump-in. The jump-in is from the relatively short range attractive van der Waals force component of the force curve, where the jump-in distance,  $D_j$ , is on the order of a few nanometers. Therefore, to suppress jump-in and cause wrapping of the deformable liquid–liquid interface around the colloidal probe only requires a film a few nanometers thick between the interfaces. The van der Waals force between an oil drop and a silica particle in an electrolyte solution is effectively constant for a specific oil,<sup>33</sup> thus the variable portion of the surface force is the EDL force which can alter through changing the surface potential and Debye length. The surface potential represents the overall magnitude of the repulsion while the Debye length represents the range of the force. If the Debye length is held constant, a decrease in surface potential results in a decrease in the force at which jump-in occurs. For the same drop parameters with a constant surface potential of at least 30 mV, a decrease in the Debye length results in an increase in the jump-in force and eventually leads to wrapping.

A comparison of these effects independently is not always applicable since in many systems the surface potential,  $\Psi_0$ , is coupled to the Debye length,  $\kappa^{-1}$ , where a decrease in  $\kappa^{-1}$  corresponds to a decrease in  $\Psi_0$  (as is the observed case for silica<sup>34</sup> and butyl acetate<sup>21</sup>). This leads to competing effects on the force behavior, where holding  $\Psi_0$  constant and decreasing  $\kappa^{-1}$  leads to wrapping, whereas holding  $\kappa^{-1}$  constant and decreasing  $\Psi_0$  leads to jump-in.<sup>19</sup> While the above two competing effects can determine the jump-in or wrapping behavior it is important to note from eqn. (4) that the interfacial tension can overshadow the EDL effects. In the presence of a short range attraction and a large interfacial tension, jump-in is expected because the interface does not easily deform (this occurs when the EDL disjoining pressure is too small to satisfy eqn. (4)). Yet, for the same disjoining pressure, wrapping may be observed if the interfacial tension is sufficiently low. When all three effects are comparable, the expected DLVO behavior may be system dependent.

### Predicting the force curve

The predictive model employed here uses the semi-analytical theoretical analysis of Chan *et al.*<sup>10</sup> and Dagastine and White<sup>19</sup> to calculate the force curve,  $F(\Delta X)$ , parametric in the minimum surface separation,  $D_0$  (*i.e.*  $F(D_0)$  and  $\Delta X(D_0)$  are calculated, then  $F(\Delta X)$  can be plotted. The modeling approach requires the wetting properties of the drop (interfacial tension,  $\gamma$ , and contact angle,  $\theta_c$ ) and the particle and undistorted drop radii. To predict the force curve requires the construction of a force model in the form of a disjoining pressure (or the pressure between two flat interfaces) based on some type of force model with adjustable parameters. This approach is limited if the observed force does not have a well characterized force model, *e.g.* a specific ion effect.

The construction of a DLVO based disjoining pressure for the butyl acetate–silica interaction was accomplished by using literature values for the surface potential for each interface, given in Table 3. Electrophoresis measurements for butyl acetate drops as a function of sodium chloride concentration are available from Stevens *et al.*<sup>21</sup> The analysis of electrophoretic mobility measurements of liquid droplets without any added stabilizer or surfactant is complicated by the possibility of internal flow in the drop. This effect results in a larger electrophoretic mobility for a droplet compared to a rigid particle of the same size and zeta potential.<sup>35</sup> Whereas the presence of stabilizers has been shown to arrest this phenomenon,<sup>36</sup> Stevens *et al.*<sup>21</sup> did not address this possibility in their

**Table 3** The infinite separation surface potentials,  $\Psi_0^\infty$ , for silica<sup>34</sup> and butyl acetate<sup>21</sup> as a function of electrolyte concentration used for the EDL calculations

Concentration/mM	$\Psi_0^\infty$ /mV, butyl acetate	$\Psi_0^\infty$ /mV, silica
0.1	30.0	65
1.0	29.6	58
10.0	26.5	43

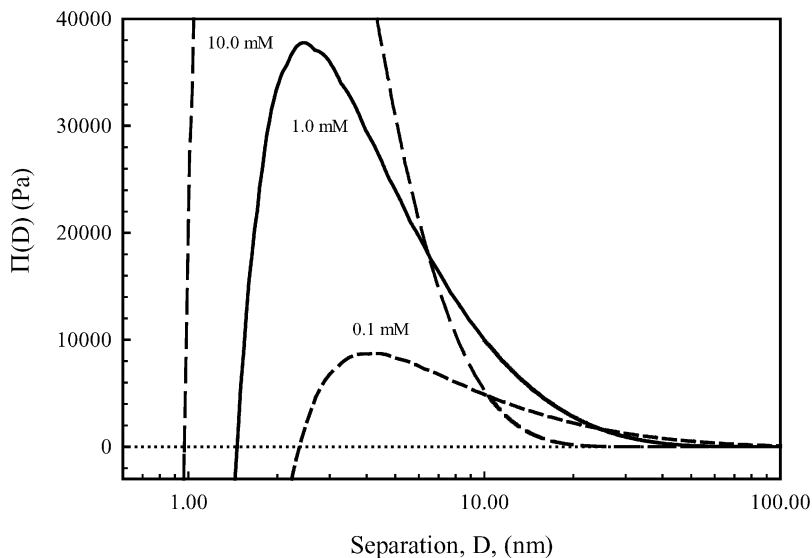


**Fig. 8** The DLVO disjoining pressure between flat interfaces constructed from the sum of the retarded van der Waals interaction calculated using Lifshitz theory between an alkane and silica across a water with electrolyte and an EDL force from a numerical solution to the Poisson–Boltzmann equation with a constant surface charge boundary condition. The short dashed, solid, and long dashed lines correspond to 0.1 mM, 1.0 mM and 10.0 mM ionic strengths.

study, thus their mobility measurements may have overestimated the zeta potential on the droplets. Surface potential data for the silica probe were used from AFM colloidal probe measurements<sup>34</sup> in inorganic electrolyte solutions. It is possible that the saturated solutions of butyl or octyl acetate

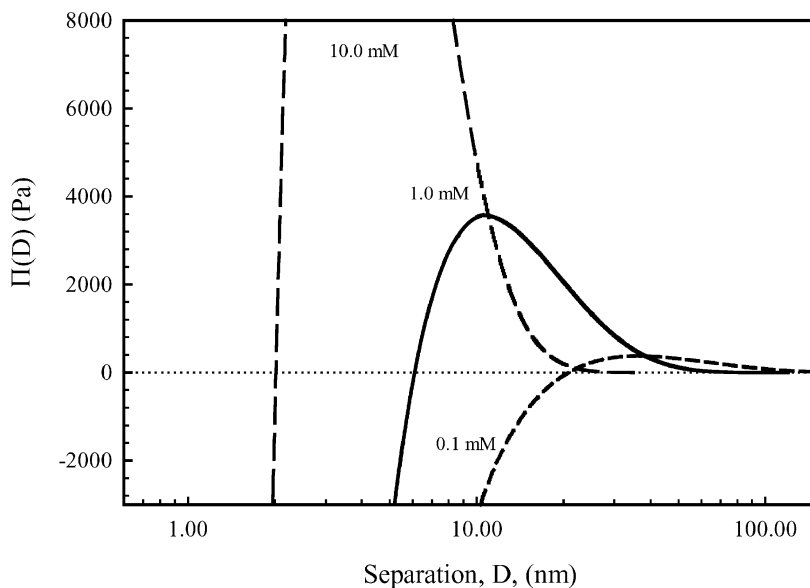


**Fig. 9** The DLVO disjoining pressure between flat interfaces constructed from the sum of the retarded van der Waals interaction calculated using Lifshitz theory between an alkane and silica across a water with electrolyte and an EDL force from a numerical solution to the Poisson–Boltzmann equation with a constant surface potential boundary condition. The short dashed, solid, and long dashed lines correspond to 0.1, 1.0 and 10.0 mM ionic strengths.

used in this study may have lowered the silica zeta potential, but this should be a small effect. The EDL force was calculated by solving the Poisson–Boltzmann equation numerically using the algorithm of Chan *et al.*<sup>37</sup> for both constant charge and constant potential boundary conditions. These two cases bracket most types of EDL behavior. The van der Waals force was predicted by calculating the retarded Hamaker constant for silica interacting with an alkane across water in an electrolyte solution, using Lifshitz theory.<sup>33</sup> An alkane was used for the butyl acetate in the van der Waals calculation because the complete dielectric spectrum of butyl acetate was not available. The dielectric spectra used in the van der Waals calculation for water, silica and the alkane were from Dagastine *et al.*,<sup>38</sup> Hough and White,<sup>39</sup> and Parsegian and Weiss.<sup>40</sup> The resulting disjoining pressures are given in Figs. 8 and 9 for the constant surface charge (CP) and constant surface potential (CP) boundary conditions, respectively.

Predicted force–separation curves for three ionic strengths are given in Figs. 10 and 11 for the CC and CP boundary conditions. The  $\Delta X_{\text{th}}$  ( $= X - X_{\infty}$ ) in Figs. 10 and 11 is in terms of an absolute distance where  $X_{\infty}$  is the height of the undistorted drop interface at the center. This differs from  $\Delta X$  for the experimental curves by an unknown constant. For the CC case, jump-in is only seen at 0.1 mM ionic strength and wrapping occurs at the other ionic strengths. In the constant potential case, jump-in is observed for the 0.1 mM and 1 mM ionic strengths, but wrapping occurs for the 10 mM ionic strength. The constant potential boundary conditions result in larger attractive disjoining pressures from the dissimilar surface potentials, where charge reversal occurs, thereby increasing the total attractive force. The wrapping thickness and jump-in distances are not known for the experimental data, but the model calculations allow estimations of their values because the predicted force curves were calculated parametric in separation distance,  $D_0$ , (*i.e.*  $F(D_0)$  and  $\Delta X(D_0)$ ). The calculated jump-in distances range from 2 nm to 4 nm and the wrapping distances range from 5 nm to 8 nm for the model force curves.

The wrapping behavior for the 1 mM and 10 mM ionic strengths in Fig. 10 is a product of the change in Debye length coupled with the low interfacial tension. The surface potential on the butyl acetate drop does not vary significantly with ionic strength (See Table 3). Therefore, this is similar to the discussion in the previous section where the surface potential was held constant and wrapping occurred as the Debye length decreased. It was also noted earlier that the surface potentials for the

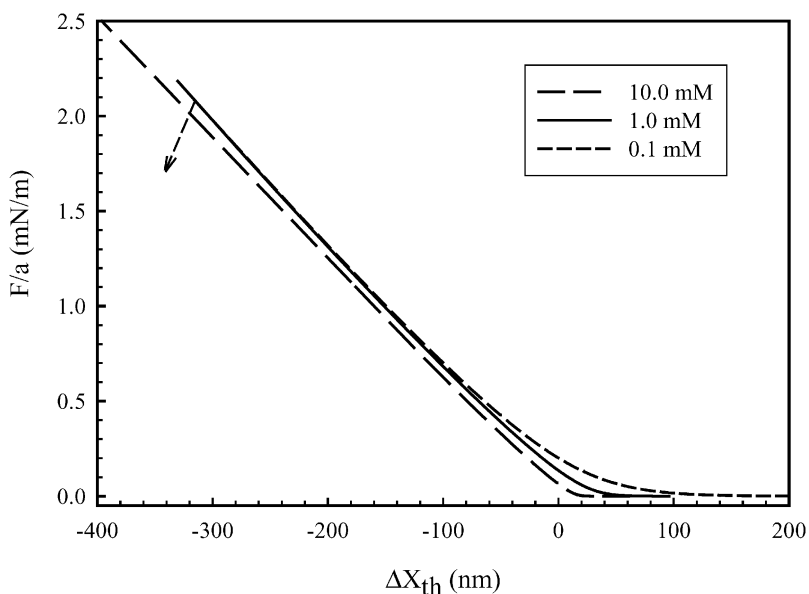


**Fig. 10** The predicted force curves between a butyl acetate droplet and a silica sphere as a function of ionic strength were calculated using the semi-analytical model with independently measured drop parameters ( $\gamma = 13.5 \text{ mN m}^{-1}$ ,  $\theta_c = 140^\circ$ ) and the DLVO disjoining pressure given in Fig. 8 for constant surface charge boundary conditions for the EDL force. The arrow denotes jump-in for the 0.1 mM ionic strength.

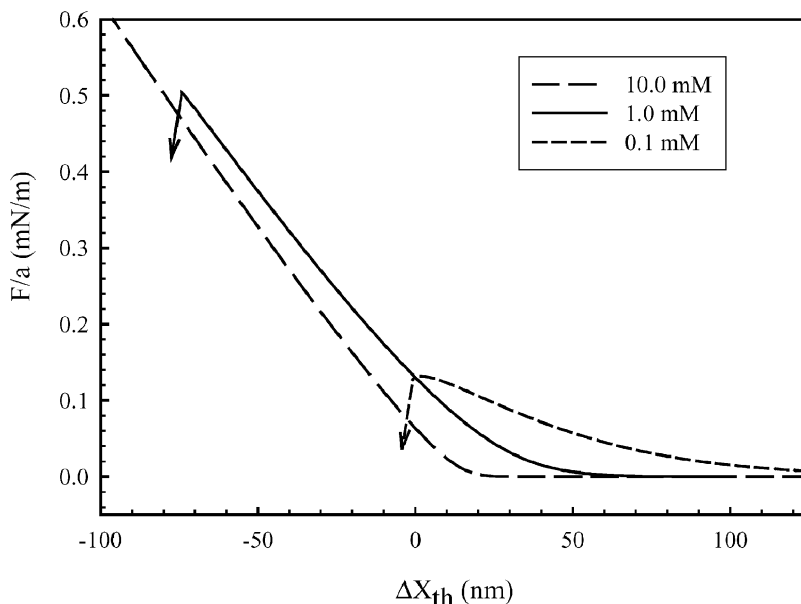


**Fig. 11** The predicted force curves between a butyl acetate droplet and a silica sphere as a function of ionic strength were calculated using the semi-analytical model with independently measured drop parameters ( $\gamma = 13.5 \text{ mN m}^{-1}$ ,  $\theta_c = 140^\circ$ ) and the DLVO disjoining pressure given in Fig. 9 for constant surface potential boundary conditions for the EDL force. The arrows denote jump-in for the 0.1 mM and 1.0 mM ionic strengths.

butyl acetate may be an over estimate, but decreasing the surface potential by approximately 10 mV did not vary the outcome for any of the force curves where wrapping was observed. A significant increase in interfacial tension (on the order of  $20 \text{ mN m}^{-1}$ ) is required to see jump-in behavior.

These predictions are in contrast to the DLVO behavior observed for force measurements with alkane droplets, where jump-in was observed experimentally and the force at jump-in decreased with ionic strength.<sup>8,11,18</sup> A van der Waals attraction is the expected source of the jump-in and this attraction alone leads to jump-in distances of only several nanometers. The force curve termination behavior in the alkane systems was governed by the change in surface potential as discussed in the previous section. The interfacial tension of alkanes is on the order of  $50 \text{ mN m}^{-1}$ , which is four times the interfacial tension for butyl acetate in water. Thus, wrapping would be observed if the interfacial tension had been significantly lowered. Wrapping behavior has been observed with alkanes by several investigators upon the addition of anionic surfactant to the alkane–water interface.<sup>8,11,12,17,18</sup> The present work is the first to study the wrapping and jump-in behaviors with organic liquids without stabilizers at considerably lower interfacial tensions than previously investigated.

### Model-experiment comparison

The force measurements in sodium nitrate solution compare well to the predicted force curves with a constant charge boundary condition. The experimental force curve at 0.1 mM electrolyte does not show jump-in, but the predicted jump-in force for the CC boundary condition is larger than the experimental range measured. Wrapping was observed for 1 mM and 10 mM concentrations at all measured forces. This semi-quantitative agreement does not guarantee that the CC boundary condition is met and charge regulation may be possible (resulting in a surface boundary condition intermediate between the CC and CP cases), but the presence of wrapping implies that the CP boundary condition behavior is not observed. Therefore, the comparison of the sodium nitrate data to the model for butyl acetate does indicate that the force follows a DLVO type behavior. This force behavior for octyl acetate is also consistent with the DLVO force model, where the interfacial tension is only  $5 \text{ mN m}^{-1}$  greater and the polar organic liquid is insoluble in water.

Whereas the sodium nitrate solution force data follows the expected DLVO behavior, simply changing the electrolyte leads to jump-in at all concentrations for both the calcium nitrate and sodium perchlorate systems with both butyl and octyl acetate. As discussed above, all the other experimental parameters were constant other than the type of electrolyte used. Although the predicted force curves for the CP boundary condition predict jump-in for the lower two ionic strengths, the force at jump-in increases in the model calculations, whereas the force at jump-in decreases in the experimental data. The observed force behavior for these two electrolytes is similar to the behavior observed in alkanes, but to explain this behavior in terms of the DLVO force model would require an increase, by a factor of 3 to 4, in the interfacial tension. This was not observed in pendant drop measurements that were made on these solutions. Therefore, with the available electrokinetic data, it is clear that the behavior of the sodium perchlorate and calcium nitrate force measurements do not follow the expected DLVO behavior for either the butyl or octyl acetate force measurements.

The presence of the strong attraction forces with the calcium nitrate and sodium perchlorate systems cannot be explained by just DLVO forces alone. The multivalent calcium ion will screen the EDL double layer forces to a larger extent at the same concentrations as the other electrolytes, but the ionic strengths are still of the same order of magnitude. The sodium perchlorate data would be expected to match the sodium nitrate data without significant variation. The calcium nitrate and sodium perchlorate behavior gives rise to an unexplained attraction that must be large enough to overcome the EDL force. Since the predicted wrapping distances are on the order of 5 nm to 10 nm, this force is not necessarily long range. It is difficult to speculate on the origins of this force behavior, other than it is a specific ion effect that results in a non-DLVO attraction. The origin of this effect may be from molecular ordering at either interface or charge regulation driven by a specific ion effect on either interface, but this cannot be determined for the force measurements. It should be noted that non-DLVO forces as found in this study have not been observed in silica-silica interactions; therefore the source of the attraction probably resides with the liquid-liquid interface.

## Conclusions

The attractive forces observed in aqueous solutions between a silica sphere and butyl or octyl acetate droplets in the presence of sodium perchlorate and calcium nitrate cannot be explained with the current DLVO theory for colloidal forces. Force measurements for the same systems with sodium nitrate were consistent with DLVO predictions. This indicates that the origin of this non-DLVO force on the length scale of 5 nm to 10 nm is manifestation of a specific ion effect. The origins of this effect may be a specific ion charge regulation mechanism or some type of molecular structure at the liquid-liquid interface. However, this speculation cannot be elucidated from the force data and is an area for further study.

## Acknowledgements

This work was supported by the Australian Research Council and by the National Science Foundation under Grant No. INT-0202675.

## References

- 1 B. V. Derjaguin, N. V. Churaev and V. M. Muller, *Surface Forces*, Consultant Bureau, New York, 1987.
- 2 R. Aveyard, B. P. Binks, W. G. Cho, L. R. Fisher, P. D. I. Fletcher and F. Klinkhammer, *Langmuir*, 1996, **12**, 6561.
- 3 B. P. Binks, W. G. Cho and P. D. I. Fletcher, *Langmuir*, 1997, **13**, 7180.
- 4 P. Omarjee, A. Espert, O. Mondain-Monval and J. Klein, *Langmuir*, 2001, **17**, 5693.
- 5 O. Mondain-Monval, A. Espert, P. Omarjee, J. Bibette, F. Leal-Calderon, J. Philip and J. F. Joanny, *Phys. Rev. Lett.*, 1998, **80**, 1778.
- 6 W. A. Ducker, Z. G. Xu and J. N. Israelachvili, *Langmuir*, 1994, **10**, 3279.
- 7 M. L. Fielden, R. A. Hayes and J. Ralston, *Langmuir*, 1996, **12**, 3721.
- 8 P. Mulvaney, J. M. Perera, S. Biggs, F. Grieser and G. W. Stevens, *J. Colloid Interface Sci.*, 1996, **183**, 614.
- 9 M. Preuss and H.-J. Butt, *J. Colloid Interface Sci.*, 1998, **208**, 468.

- 10 D. Y. C. Chan, R. R. Dagastine and L. R. White, *J. Colloid Interface Sci.*, 2001, **236**, 141.
- 11 D. E. Aston and J. C. Berg, *J. Colloid Interface Sci.*, 2001, **235**, 162.
- 12 R. R. Dagastine, D. C. Prieve and L. R. White, *J. Colloid Interface Sci.*, 2004, **269**, 84.
- 13 R. R. Dagastine, G. W. Stevens, D. Y. C. Chan and F. Grieser, *J. Colloid Interface Sci.*, 2004, **273**, 339.
- 14 D. Bhatt, J. Newman and C. J. Radke, *Langmuir*, 2001, **17**, 116.
- 15 H.-J. Butt, *J. Colloid Interface Sci.*, 1994, **166**, 109.
- 16 G. Gillies, C. A. Prestidge and P. Attard, *Langmuir*, 2001, **17**, 7955.
- 17 S. A. Nespolo, D. Y. C. Chan, F. Grieser, P. G. Hartley and G. W. Stevens, *Langmuir*, 2003, **19**, 2124.
- 18 P. G. Hartley, F. Grieser, P. Mulvaney and G. W. Stevens, *Langmuir*, 1999, **15**, 7282.
- 19 R. R. Dagastine and L. R. White, *J. Colloid Interface Sci.*, 2002, **247**, 310.
- 20 P. Attard and S. J. Miklavcic, *J. Colloid Interface Sci.*, 2002, **247**, 255.
- 21 G. W. Stevens, H. R. C. Pratt and D. R. Tai, *J. Colloid Interface Sci.*, 1990, **136**, 470.
- 22 S. Abid and A. K. Chesters, *Int. J. Multiphase Flow*, 1994, **20**, 613.
- 23 E. Klaseboer, J. P. Chevaillier, C. Gourdon and O. Masbernat, *J. Colloid Interface Sci.*, 2000, **229**, 274.
- 24 J. N. Connor and R. G. Horn, *Langmuir*, 2001, **17**, 7194.
- 25 D. G. Goodall, M. L. Gee, G. Stevens, J. Perera and D. Beaglehole, *Colloids Surf., A*, 1998, **143**, 41.
- 26 W. A. Ducker, T. J. Senden and R. M. Pashley, *Nature*, 1991, **353**, 239.
- 27 H. J. Butt, *Biophys. J.*, 1991, **60**, 1438.
- 28 P. Attard and S. J. Miklavcic, *Langmuir*, 2001, **17**, 8217.
- 29 E. J. W. Verwey and J. T. G. Overbeek, *Theory of Stability of Lyophobic Colloids*, Elsevier, Amsterdam, 1948.
- 30 B. V. Derjaguin and L. Landua, *Acta Physicochim. USSR*, 1941, **14**, 633.
- 31 J. L. Hutter and J. Bechhoefer, *Rev. Sci. Instrum.*, 1993, **64**, 1868.
- 32 R. J. Hunter, *Foundations of Colloid Science*, Clarendon Press, Oxford, 1995.
- 33 J. Mahanty and B. W. Ninham, *Dispersion Forces*, Academic Press, London, 1976.
- 34 W. A. Ducker, T. J. Senden and R. M. Pashley, *Langmuir*, 1992, **8**, 1831.
- 35 H. Ohshima, T. W. Healy and L. R. White, *J. Chem. Soc., Faraday Trans. 2*, 1984, **80**, 1643.
- 36 S. A. Nespolo, M. A. Bevan, D. Y. C. Chan, F. Grieser and G. W. Stevens, *Langmuir*, 2001, **17**, 7210.
- 37 D. Y. C. Chan, R. M. Pashley and L. R. White, *J. Colloid Interface Sci.*, 1980, **77**, 283.
- 38 R. R. Dagastine, D. C. Prieve and L. R. White, *J. Colloid Interface Sci.*, 2000, **231**, 351.
- 39 D. B. Hough and L. R. White, *Adv. Colloid Interface Sci.*, 1980, **14**, 3.
- 40 V. A. Parsegian and G. H. Weiss, *J. Colloid Interface Sci.*, 1981, **81**, 285.